BAMS Article

West Coast Forecast Challenges and Development of Atmospheric River Reconnaissance

F. Martin Ralph, Forest Cannon, Vijay Tallapragada, Christopher A. Davis, James D. Doyle, Florian Pappenberger, Aneesh Subramanian, Anna M. Wilson, David A. Lavers, Carolyn A. Reynolds, Jennifer S. Haase, Luca Centurioni, Bruce Ingleby, Jonathan J. Rutz, Jason M. Cordeira, Minghua Zheng, Chad Hecht, Brian Kawzenuk, and Luca Delle Monache

ABSTRACT: Water management and flood control are major challenges in the western United States. They are heavily influenced by atmospheric river (AR) storms that produce both beneficial water supply and hazards; for example, 84% of all flood damages in the West (up to 99% in key areas) are associated with ARs. However, AR landfall forecast position errors can exceed 200 km at even 1-day lead time and yet many watersheds are <100 km across, which contributes to issues such as the 2017 Oroville Dam spillway incident and regularly to large flood forecast errors. Combined with the rise of wildfires and deadly post-wildfire debris flows, such as Montecito (2018), the need for better AR forecasts is urgent. Atmospheric River Reconnaissance (AR Recon) was developed as a research and operations partnership to address these needs. It combines new observations, modeling, data assimilation, and forecast verification methods to improve the science and predictions of landfalling ARs. ARs over the northeast Pacific are measured using dropsondes from up to three aircraft simultaneously. Additionally, airborne radio occultation is being tested, and drifting buoys with pressure sensors are deployed. AR targeting and data collection methods have been developed, assimilation and forecast impact experiments are ongoing, and better understanding of AR dynamics is emerging. AR Recon is led by the Center for Western Weather and Water Extremes and NWS/NCEP. The effort's core partners include the U.S. Navy, U.S. Air Force, NCAR, ECMWF, and multiple academic institutions. AR Recon is included in the "National Winter Season Operations Plan" to support improved outcomes for emergency preparedness and water management in the West.

https://doi.org/10.1175/BAMS-D-19-0183.1
Corresponding author: Forest Cannon, fcannon@ucsd.edu
In final form 7 April 2020

AFFILIATIONS: **Ralph, Cannon, Wilson, Zheng, Hecht, Kawzenuk, and Monache**—Center for Western Weather and Water Extremes, Scripps Institution of Oceanography, University of California, San Diego, La Jolla, California; **Tallapragada**—NOAA/NWS/NCEP/Environmental Modeling Center, College Park, Maryland; **Davis**—National Center for Atmospheric Research, Boulder, Colorado; **Doyle and Reynolds**—U.S. Naval Research Laboratory, Monterrey, California; **Pappenberger, Lavers, and Ingleby**—European Centre for Medium-Range Weather Forecasts, Reading, United Kingdom; **Subramanian**—University of Colorado Boulder, Boulder, Colorado; **Haase and Centurioni**—Scripps Institution of Oceanography, University of California, San Diego, La Jolla, California; **Rutz**—NOAA/NWS/Western Region Headquarters, Salt Lake City, Utah; **Cordeira**—Plymouth State University, Plymouth, New Hampshire

Atmospheric rivers (AR) are long narrow corridors of water vapor transport that serve as the primary mechanism to advect moisture into midlatitude continental regions, including the U.S. West Coast (Zhu and Newell 1998; Ralph et al. 2004, 2006; Neiman et al. 2008). ARs yield beneficial impacts as their associated precipitation comprises a majority of western U.S. precipitation, including up to 50% of California's annual water supply (Dettinger 2013), but have also been responsible for nearly all major flooding events in many western watersheds (e.g., Ralph et al. 2006) and 84% of all flood insurance claims in the West over the past 40 years (up to 99% in key areas; Corringham et al. 2019). As a result, considerable effort has been dedicated to understanding AR physics, dynamics, and predictability in recent years, to both maximize the potential benefits of these systems through effective water management and minimize their hazardous impacts (Ralph et al. 2017).

Despite recent advances in understanding the importance of ARs to global moisture fluxes and regional water resources, forecasting these features remains a challenge due in part to their formation and propagation over the ocean, where in situ and surface-based observations are extremely limited (Ralph et al. 2013; Cannon et al. 2017). Although advancements in satellite data assimilation (English et al. 2013), including all-sky radiances (Zhu et al. 2016), have greatly improved global model forecast skill, the information assimilated into numerical weather prediction (NWP) models remains limited and error prone in regions of deep clouds and precipitation collocated with the AR. Furthermore, fundamental questions remain regarding the evolution of these systems that necessitate data at scales not adequately simulated by models or observed by satellites (e.g., Demirdjian et al. 2020a). Neiman et al. (2016) utilized offshore dropsonde observations of an AR during the 2014 CalWater Field Campaign (Ralph et al. 2016) to document three-dimensional thermodynamic and kinematic characteristics of an AR and its subsequent hydrometeorological impacts across Northern California from 7 to 10 February 2014, which included prolonged precipitation and moderate flooding. The impacts associated with that event were attributed to mesoscale circulations that stalled the synoptic-scale front and AR propagation, and their research contended that augmented airborne monitoring of offshore ARs is necessary to improve the understanding of the dynamic and thermodynamic processes in cloud obscured regions, which play a dominant role in AR evolution. Multiple studies have also argued that improving estimates of the initial atmospheric state in NWP models in AR conditions has the potential to improve forecasts of high-impact precipitation events (Doyle et al. 2014; Ralph et al. 2014; Neiman et al. 2016; Cordeira et al. 2017; Reynolds et al. 2019; Demirdjian et al. 2020b; for an overview of targeted observations, see Majumdar 2016). To this end, Atmospheric River Reconnaissance (AR Recon) represents an important research and operations partnership between multiple academic institutions, state and federal agencies, and stakeholders to improve forecasting of high-impact winter weather in the western United States.

AR Recon supports the improved prediction of landfalling ARs on the U.S. West Coast by supplementing conventional data assimilation with targeted dropsonde observations of atmospheric profiles of water vapor, temperature, and winds within ARs. The concept for AR Recon was first recommended in a 2013 report to the Western States Water Council that was prepared by a broad cross-disciplinary group (Ralph et al. 2014). The 2016, 2018, 2019, and 2020 AR Recon campaigns took place from late January through mid-March and involved a team of scientists from multiple academic institutions, operational forecasting centers, and federal agencies. Over each winter season that AR Recon has been executed, the campaign has utilized a combination of available aircraft: the National Oceanic and Atmospheric Administration (NOAA) Gulfstream IV (G-IV) and two U.S. Air Force (USAF) C-130s, which are strategically stationed ahead of events to collectively cover wide swaths of the eastern Pacific for broad sampling of AR features (Fig. 1). Ongoing work to quantify the impact of targeted observations on forecast skill in the western United States and its potential value to regional stakeholders is an essential part of establishing the cost effectiveness and operational potential of continued observational targeting in ARs (e.g., Hamill et al. 2013; Parsons et al. 2017). While the reported impact of targeted observations in the literature to date has been marginal (Majumdar et al. 2016), a thorough investigation of the value of targeted AR observations to western U.S. forecast challenges has yet to be carried out. Furthermore, recent investigations specific to this problem (e.g., Lavers et al. 2018; Wick et al. 2018; Kren et al. 2018; Stone et al. 2020; Schindler et al. 2020) have demonstrated a consistent positive impact of targeted dropsonde observations on operational forecasts that warrants continued research investment.

This manuscript is intended to define the need for AR Recon, detail the execution of the campaign in recent seasons, and introduce ongoing work to determine the impact of AR Recon on western U.S. forecast skill. The second section provides an overview of unique forecast challenges for the U.S. West Coast. The third section describes the basic organization of AR Recon and its primary sponsors. The fourth section details AR forecasting and observation targeting during the campaign, and the fifth section describes the execution of the campaign in recent winter seasons. The sixth section introduces a formal steering committee on AR Recon NWP modeling and data assimilation, and briefly highlights studies to determine the impact of the campaign on West Coast forecast skill. The final section discusses the ongoing transition of AR Recon from a research program to a research and operations partnership as

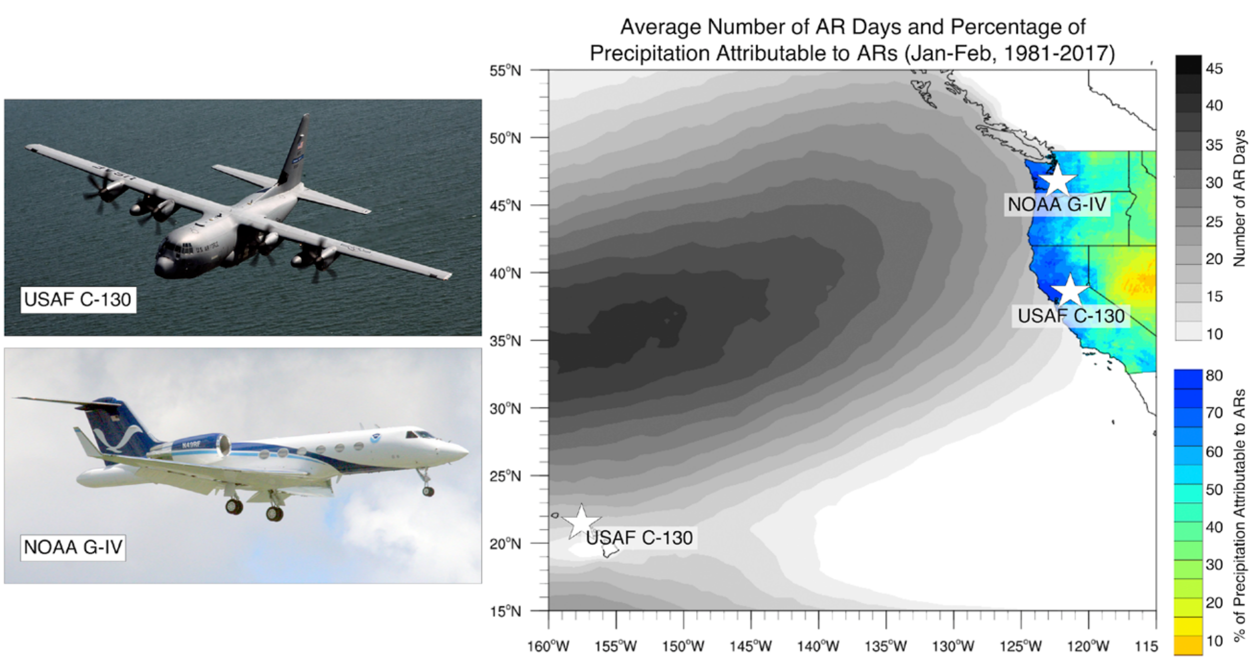

Fig. 1. Staging locations of USAF and NOAA Aircraft that participated in AR Recon 2018 (white stars), climatological frequency of ARs during January and February (grayscale), and percentage of winter-season precipitation contributed by ARs (color fill). Only the USAF aircraft were available in 2019.

part of the Office of the Federal Coordinator for Meteorology (OFCM) National Winter Season Operations Plan (NWSOP) (OFCM 2019).

U.S. West Coast forecast challenge examples

Flood forecasting. The challenge of predicting most floods in the western states results primarily from errors in forecasts of precipitation, which in turn are closely related to errors in the prediction of ARs. Although western U.S. forecasting of floods and of the precipitation that causes them has improved over time, major gaps remain at 0–4-day lead time that limit decision support for water management and hazard mitigation (Sukovich et al. 2014; Lavers et al. 2016). Many of these challenges result from errors in the prediction of AR landfall position, intensity, orientation, duration (Wick et al. 2013; Lavers et al. 2016; Cordeira et al. 2017; DeFlorio et al. 2018; Nardi et al. 2018; Martin et al. 2018), and temperature (White et al. 2010; Henn et al. 2020).

A notable example of hydrologic forecast challenges occurred ahead of moderate flooding on 15 February 2019 on the Russian River in coastal Northern California. The river crested at 35 ft (3 ft above flood stage; 1 ft ≈ 0.305 m; Fig. 2) at Guerneville, CA (the most flood-prone location in the western United States; Ralph et al. 2006), though the California Nevada River Forecast Center (CNRFC) forecast issued 1.5 days earlier was for 39 ft (7 ft above flood stage), and was cause for evacuation preparations. The forecasted stage 4 days prior to the crest was only 25 ft—a forecast range of 14 ft within 4 days of the event. A subsequent AR on 26–27 February 2019 impacting the saturated watershed generated the largest flood on the Russian River since 2005 (46-ft stage height; not shown), but the peak was underforecast by approximately 14 ft 4 days prior. These examples are not only current, but also representative. In a 2017 AR event impacting the Russian River forecast variability within 0–4-day lead time was 13 ft, and in a well-documented AR case in 2014 it was 11 ft (Martin et al. 2018). The stage-height forecast range between 0- and 4-day lead time across all eight cases exceeding monitor stage (29 ft) at Guerneville from 2011 to 2019 exceeded 10 ft (not shown). These rapid changes in flood forecasts are not uncommon throughout the West due to uncertainties in precipitation forecasts at short lead times, which are most often associated with challenges in predicting AR landfall characteristics (e.g., location, intensity, and duration; Ralph et al. 2019).

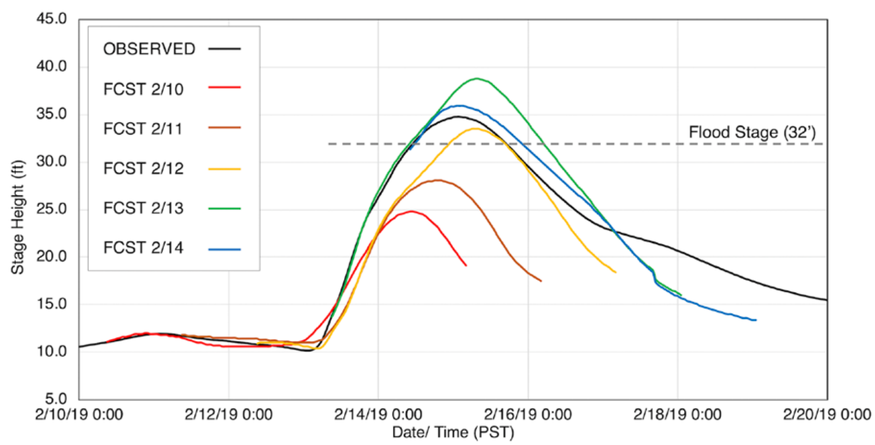

Fig. 2. Time series of CNRFC stage-height forecasts issued at 0.5–4.5-day lead time ahead of peak stage height at the Guerneville gauge on the Russian River in coastal Northern California on 15 Feb 2019. Flood stage for the Russian River is 32 ft (dashed gray line).

AR forecasting challenges. Global NWP skill in predicting AR characteristics has primarily been investigated at the synoptic scale, where ARs are a recognizable feature of the extratropical circulation (Wick et al. 2013; Guan and Waliser 2015; DeFlorio et al. 2018). However, it is recognized that mesoscale phenomena associated with AR evolution also create challenges in forecasting their impacts at short lead time (Leung and Qian 2009; Neiman et al. 2009; Ralph et al. 2013; Cannon et al. 2018; Martin et al. 2018; Cannon et al. 2020a,b; Demirdjian et al. 2020a,b). Wick et al. (2013) found forecasts of landfalling ARs to frequently err by ±400 km at 3-day lead time. While typical AR landfall location errors vary according to region and intensity, Nardi et al. (2018) also demonstrated that errors for moderate intensity and greater ARs (i.e., IVT > 500 kg m^{-1} s^{-1}) were generally on the order of several hundred kilometers at 1–3-day lead across nine operational global models. The large landfall location errors at short lead times are partially attributed to the influence of mesoscale frontal wave development in landfalling ARs (Ralph et al. 2010; Neiman et al. 2016; Martin et al. 2018). Furthermore, the magnitude of these errors are critical when considering that the extent of individual watersheds in the West is often on the scale of just 100 km (e.g., the Russian and Feather River watersheds). These findings highlight the need for significant improvement in AR forecasts at the short lead times for optimal water management and hazard mitigation outcomes in the West.

A notable example of an impactful AR that was poorly forecast at short lead times occurred on 7–11 February 2017, during the Oroville Dam Spillway Incident in Northern California that led to the evacuation of 188,000 people downstream (Schweiger 2018). While the water management challenges associated with this event were not strictly attributed to the meteorological extremes (Vano et al. 2019), the event's forecast was notably challenging. At 3-day lead time, errors in predicted AR magnitude and duration translated to uncertainty in precipitation forecasts in the northern Sierra Nevada. Specifically, the development of a mesoscale frontal wave (Ralph et al. 2010; Neiman et al. 2016; Martin et al. 2018) that prolonged IVT conditions and intensified upslope moisture transport within the watershed on 7–8 February was not forecast beyond 1-day lead time. The escalation of landfalling AR conditions along the coast from "moderate" at 2-day lead time to "strong" 1 day ahead and "extreme" at observation time [based on evaluating Global Ensemble Forecast System (GEFS) data relative to the AR scale; Ralph et al. 2018; Fig. 3] contributed to the underprediction of precipitation accumulation by more than 20% over the Feather River watershed and exacerbated challenges in water management and emergency response at Oroville. Furthermore, the sustained AR conditions were associated with elevated freezing levels that contributed to watershed-wide runoff (White et al. 2019).

A separate event that affected Southern California on 22–23 March 2018 demonstrates the impacts that overprediction of AR intensity and duration can have on quantitative precipitation forecast skill and the challenges that forecast error posed to regional emergency management (Fig. 4). At a 7-day lead time, a strong AR was predicted to broadly impact the state, including significant precipitation forecast for areas that were recently burned by the Thomas Fire in the transverse ranges of Southern California during December 2017. Quantitative precipitation forecasts predicted precipitation rates exceeding debris flow thresholds for the region at 1-day lead time. Given the forecast and the recent Montecito debris flow disaster (Oakley et al. 2018), over 30,000 residents of the South Coast region (including Montecito) were evacuated as a precautionary measure. However, the largest precipitation impacts were ultimately observed over the central coast mountains to the north, where precipitation had been underforecast, while

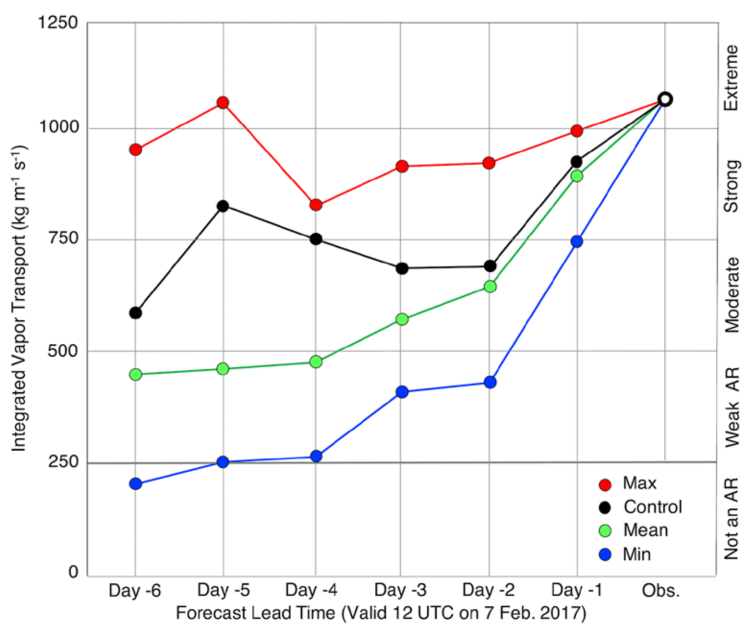

Fig. 3. GEFS IVT forecasts for a coastal grid point at 38°N during the 7–11 Feb 2017 AR that impacted the Feather River watershed. Individual dots identify the maximum (red), mean (green), and minimum (blue) values from 21 ensemble members on a given model initialization date (starting at 6-day lead time). Only the peak value within the forecast period is shown for each category. The black dots indicate the forecasted value in the deterministic run.

the Thomas Fire burn area received considerably less precipitation than predicted and rain rates below debris flow–triggering thresholds. Again, GEFS misrepresented the position, orientation, and evolution of landfalling AR conditions, even at short lead times. Specifically, the observed AR made landfall 200–250 km farther north than predicted by NOAA's deterministic Global Forecast System (GFS) initialized 24 h prior and progressed southward across Southern California with weaker vapor transport than predicted at sub-1-day lead time (Fig. 5), contributing to a 1-day precipitation forecast error of more than 100 mm. The northward shift in forecast minus observed AR landfall was consistent across all GEFS members. For both example cases, offshore observation profiles of water vapor, winds, and temperature from dropsondes within the AR may have positively impacted the simulation of the evolution of the AR, thereby improving precipitation forecast skill.

These example cases are consistent with Wick et al. (2013), which evaluated AR forecast differences across five state-of-the-art NWP modeling systems for an event that produced more than 15 in. of precipitation in 24 h in the Washington Cascades and record reservoir inflow at Howard Hanson Dam. While each model clearly predicted the occurrence of a landfalling AR, even out to 7 days, relevant characteristics such as the predicted position, width, orientation, and moisture content varied significantly across the evaluated models and lead times. Their results further demonstrated that the forecast challenges of that particular case study are representative of AR landfall predictability challenges over the entire western U.S. coast, in general, and their conclusions were influential in first recommending the concept for AR Recon to the Western States Water Council in 2013 (Ralph et al. 2014).

AR Recon organization

The AR Recon campaign is a multiyear cooperative effort to develop and test the potential of targeted airborne observations to improve forecasts of AR impacts on the U.S. West Coast at lead times of less than 5 days. The first season of AR Recon collected dropsonde observations in three ARs in February 2016 using two USAF C-130 aircraft (in coordination with the El Niño Rapid Response field campaign). The continuation of AR Recon included six intensive observation periods (IOPs) flown in January to February 2018 (including up to three aircraft; two USAF C-130s and the NOAA G-IV), six IOPs flown in February to March 2019 (using two C-130s), and 17 IOPs in January to March 2020 (using two C-130s and the G-IV). AR Recon

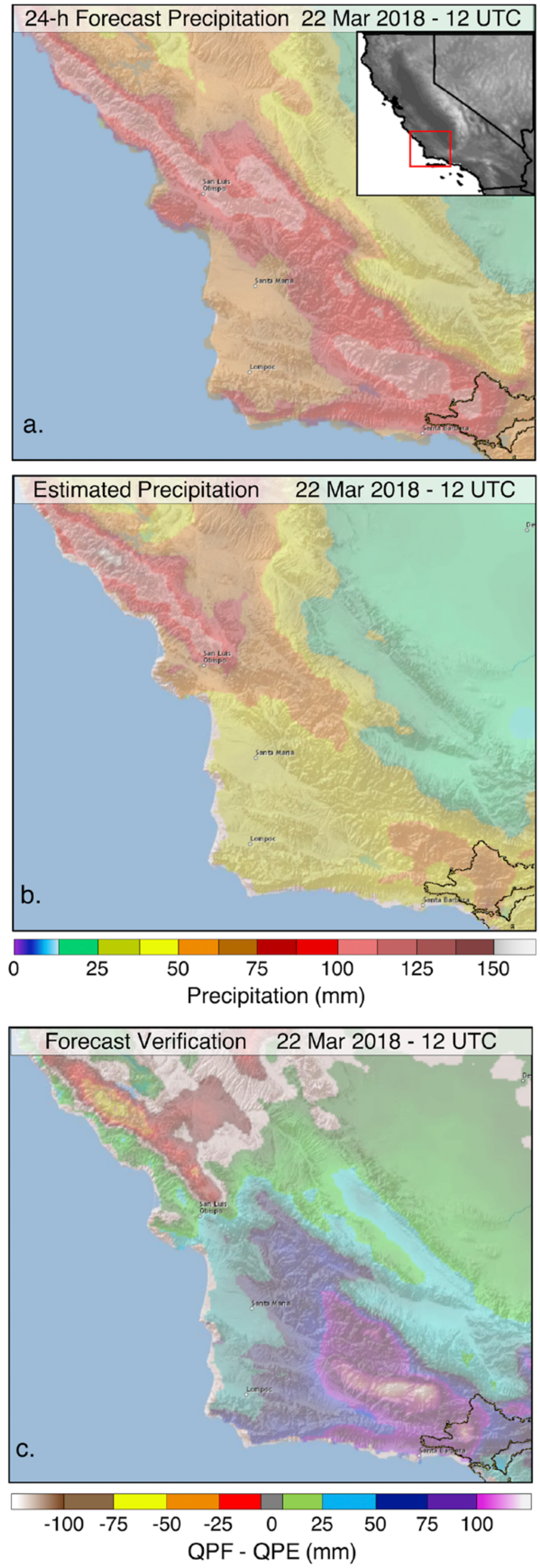

Fig. 4. (a) CNRFC 24-h quantitative precipitation forecast for central California valid at 1200 UTC 22 Mar 2018. (b) Estimated observed precipitation and (c) forecast verification (forecast minus observed). The black outline indicates the Thomas Fire burn area and a large-scale map is shown in the upper right of (a).

also implemented Global Positioning System airborne radio occultation (GPS-ARO) measurements aboard the G-IV (Haase et al. 2014) in 2018 and 2020 and deployed drifting buoys upgraded to include barometers (Centurioni et al. 2017) in 2019 and 2020 to support the project's forecast improvement objectives. Planning and execution of each AR Recon season has benefitted from accumulated experience and the continuous development and evaluation of tools and methodologies. Table 1 provides additional details about each year's campaign.

Key sponsors of AR Recon include the U.S. Army Corps of Engineers and the California Department of Water Resources, who are working with the Center for Western Weather and Water Extremes (CW3E) at Scripps Institution of Oceanography and other partners to reach their goal of using improved AR prediction to inform water and infrastructure management (e.g., Forecast Informed Reservoir Operations Steering Committee 2017). The campaign has thus far been conducted with the participation of experts on ARs, midlatitude dynamics, airborne reconnaissance, and NWP modeling, who have come together from organizations including CW3E, NOAA (National Centers for Environmental Prediction (NCEP) and National Weather Service Western Region and Aircraft Operations Center), U.S. Naval Research Laboratory (NRL), the Air Force 53rd Weather Reconnaissance Squadron, Plymouth State University, the National Center for Atmospheric Research (NCAR), the State University of New York at Albany, The University of Arizona, and the European Centre for Medium-Range Weather Forecasts (ECMWF), to participate in daily forecast discussions, flight planning, and dropsonde target identification for individual missions (e.g., Cordeira et al. 2017).

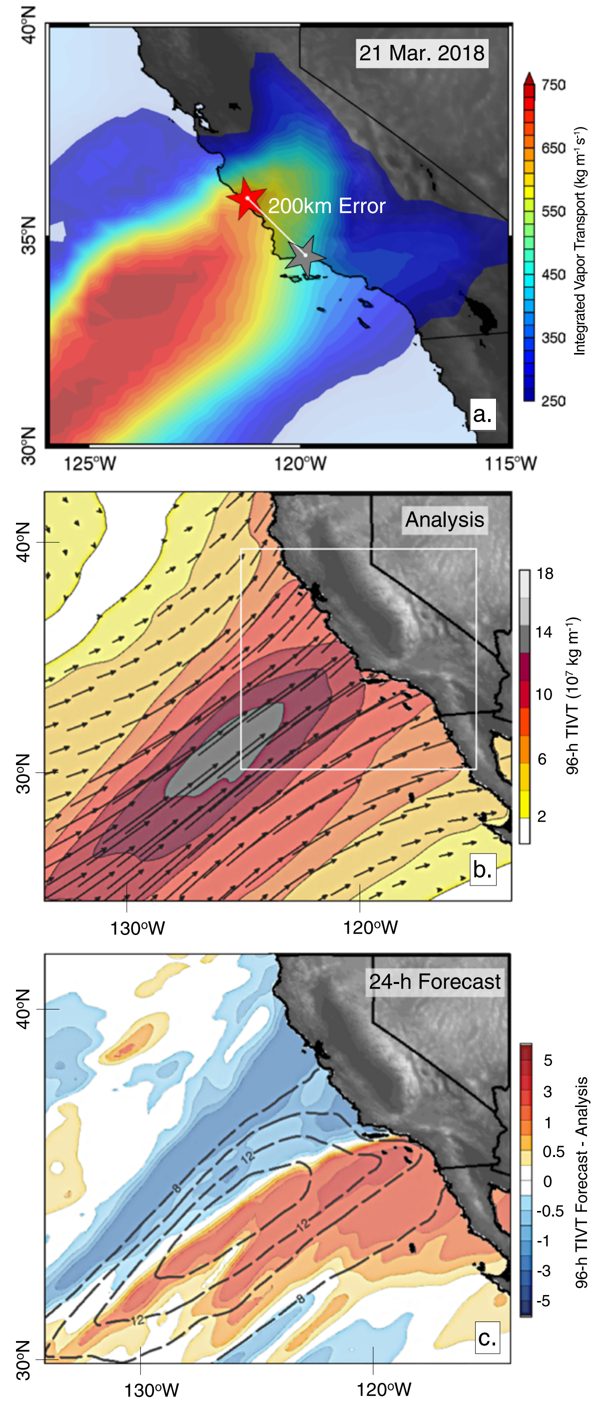

Fig. 5. (a) Landfall position of the IVT maximum for the AR impacting central and Southern California on 21–23 Mar 2018. (b) Time-integrated vapor transport (TIVT) analysis for the 96-h period beginning at 0000 UTC 20 Mar 2018 and (c) 1-day lead time TIVT forecast minus TIVT analysis for the 96-h period beginning at 0000 UTC 20 Mar 2018 (color fill) plotted over the analysis TIVT (contours).

AR Recon observation targeting

AR forecasting. The AR Recon 2016, 2018, 2019, and 2020 campaigns were conducted between late January and mid-March of each winter season, coinciding with the climatological peak of AR activity in California (Rutz et al. 2014). Daily weather briefings were provided by a collaborative team of researchers and forecasters from multiple institutions, as demonstrated by the example organizational chart for the 2018 season shown in Fig. 6, which details key individuals and their responsibilities. Weather briefings focused on 1) the current location and intensity of ARs (based on IVT and IWV) that were forecast to make landfall on the West Coast at either short-term (i.e., 1–3 days) or medium-term (i.e., 3–7 days) lead times; 2) the large-scale circulation features associated with AR conditions; 3) the probable locations and intensity of landfalling ARs in long-term (i.e., 7–10+ days) forecasts; and 4) the local weather conditions for aircraft base locations at the time of takeoff and landing. The analyses and forecasts that were used to support daily weather briefings were created from NCEP Global Forecast System (GFS) and Global Ensemble Forecast System (GEFS), NRL Coupled Ocean–Atmosphere Mesoscale Prediction System (COAMPS), and data from the ECMWF Integrated Forecasting System (IFS). Specific AR-related GFS and GEFS tools that were previously developed at CW3E were key in identifying and tracking ARs over the northeast Pacific and documenting their

Table 1. Timeline of AR Recon IOPs, aircraft staging locations, flights, and dropsondes released.

Year	No. of IOPs	Aircraft	Location	No. of flights	Total No. of sondes
2016	3	USAF C-130	Hickam AFB, Hawaii	3	272
		USAF C-130	McChord AFB, California	3	
2018	6	USAF C-130	Hickam AFB, Hawaii	5	361
		USAF C-130	Travis AFB, California	5	
		NOAA G-IV	Paine Field, Washington	3[a]	
2019[b]	6	USAF C-130	Hickam AFB (Hawaii)[c]	4	291
		USAF C-130	Travis AFB (California)[c]	5	
2020[b]	17	USAF C-130	Hickam AFB, Hawaii	8	733
		USAF C-130	West Coast Locations	13	
		NOAA G-IV	Portland, Oregon	13	
Annual[c]	24[d]	USAF C-130	West Coast (CA, OR, NV)	24[d]	1,800[d]
		USAF C-130	West Coast (CA, OR, NV)	24[d]	
		NOAA G-IV	Pacific (Hawaii)	24[d]	

[a] GPS radio occultation measurements taken aboard the NOAA G-IV.

[b] Drifting barometer buoys deployed from USAF C-130 (32 in 2019 and 64 in 2020).

[c] Both C-130 aircraft in IOP1 were staged from San Diego, CA.

[d] Planned.

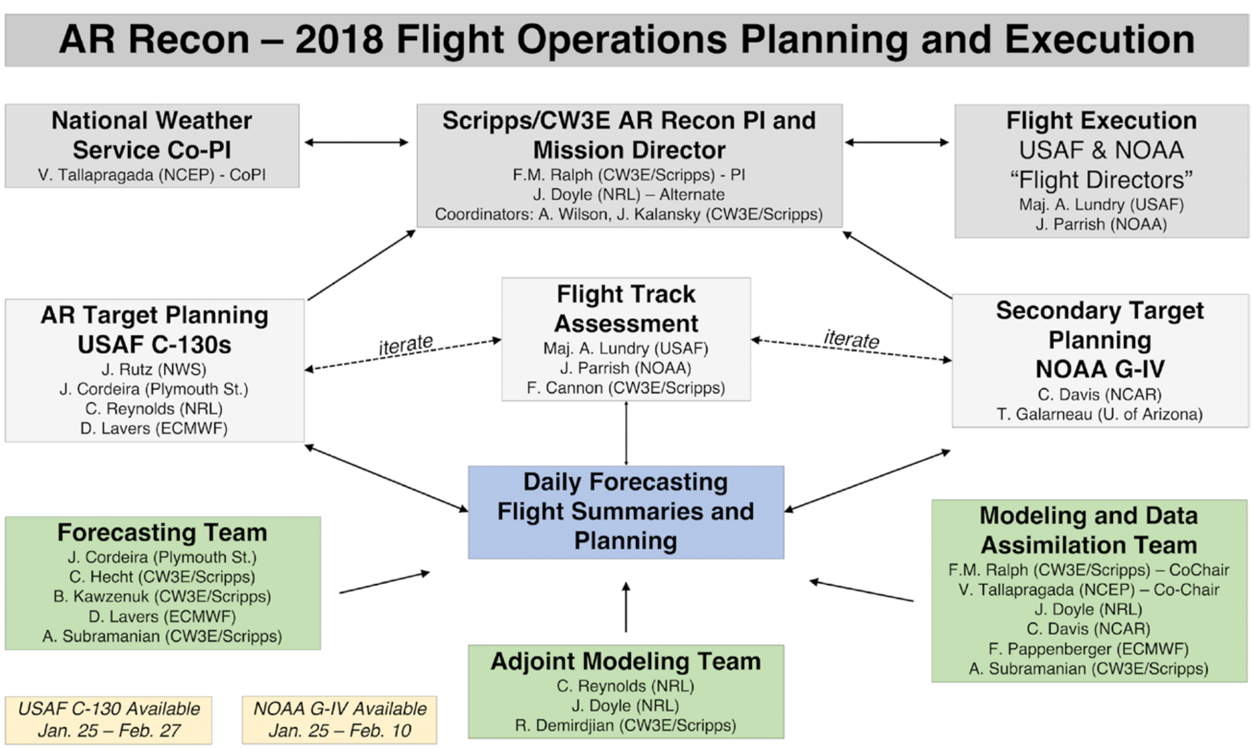

Fig. 6. Organization chart detailing participating individuals and their responsibilities during AR Recon 2018.

characteristics (e.g., structure, intensity, position, and evolution). The forecasting tools that were utilized during AR Recon are similar to those used during CalWater2 in 2015, which provided procedural guidance (Cordeira et al. 2017). Weather briefings that featured potential ARs for aircraft observation were followed by a discussion of optimal observation targets and flight-track planning.

Observation target identification. Observation target planning in the 2018, 2019, and 2020 campaigns relied upon the estimation of forecast sensitivity fields using adjoint models (e.g., Errico 1997; Doyle et al. 2012, 2014; Reynolds et al. 2019). Adjoint diagnostics have previously identified low- to midlevel moisture as a major source of sensitivity in extratropical cyclone intensification (Doyle et al. 2014, 2019), which is consistent with the importance of moist processes to the development of severe extratropical cyclones (Wernli et al. 2002), and the positive impact of the improved representation of water vapor transport on precipitation forecast skill in the western United States (Martin et al. 2018). Here, the NRL COAMPS moist adjoint model (Amerault et al. 2008; Doyle et al. 2012) was run to evaluate the sensitivity of precipitation forecasts over the West Coast to perturbations in the moisture and wind initial conditions several days prior to AR landfall (Reynolds et al. 2019).

Adjoint models allow for a mathematically rigorous calculation of forecast sensitivity of a response function to changes in initial state (Errico 1997). The gradient fields of the response function (accumulated precipitation in this case) with respect to input perturbations (e.g., moisture and winds) produced by the adjoint model have a direct interpretation as fields of "sensitivity," where the largest values have the most impact on the forecast. For example, the impact of a 1 g kg^{-1} perturbation of water vapor mixing ratio at 850 hPa in the most sensitive region, typically along the subsaturated edges of the AR (Reynolds et al. 2019), can be measured as the linear change in millimeters of precipitation over the West Coast region of interest per unit of perturbation. Doyle et al. (2014) found that extratropical cyclogenesis and precipitation forecasts for a single event were more sensitive to moisture within the associated AR than either wind or temperature, and Reynolds et al. (2019) corroborated this finding over multiple ARs impacting California during the record wet 2017 water year. Given these previous results and daily monitoring of the adjoint during three campaign seasons, water vapor sensitivity was the primary field used for observation targeting in AR Recon flight planning. However, sensitivity to midtropospheric potential vorticity perturbations was also factored into flight track planning given the importance of cyclone development on forecast evolution, especially during the 2018 and 2020 campaigns when the G-IV was available to expand AR targeting.

Figure 7 shows sensitivity of forecasted 12-h precipitation accumulations over the Pacific Northwest

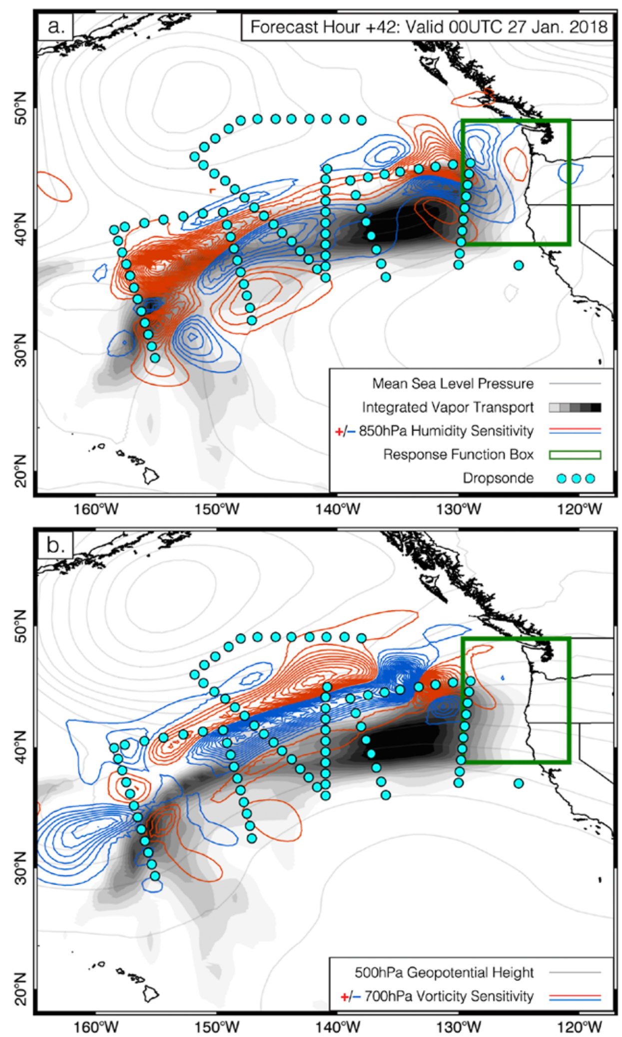

Fig. 7. COAMPS forecast sensitivity of 12-h precipitation accumulation over the Pacific Northwest 3 days later to (a) 850-hPa water vapor mixing ratio perturbations (g kg^{-1}) and (b) 700-hPa potential vorticity perturbations (PVU) at 42-h lead time ahead of IOP 1 on 27 Jan 2018.

at a 3-day lead time to 850-hPa water vapor mixing ratio perturbations (Fig. 7a) and 700-hPa potential vorticity (PV) perturbations (Fig. 7b) at the 42-h lead time ahead of IOP 1 during the 2018 season (27 January 2018). Locations of strong positive (negative) gradients in water vapor sensitivity that are found immediately north of the area of enhanced IVT indicate the regions of the forecast where initial condition perturbations were expected to have the largest positive (negative) impact on forecasted precipitation accumulations (Fig. 7a). In this specific case, the 700-hPa PV perturbation field (derived from the adjoint sensitivity) was collocated with water vapor sensitivity, indicating that precipitation accumulations over the West Coast would be most responsive to changes in AR evolution along the cold front. Subsequently, dropsonde observations were targeted to sample across these sensitive regions with the intent of providing initial conditions with the greatest potential benefit to precipitation forecast skill (Figs. 7a,b). Continuous refinement of the method for applying the adjoint and combining that information with knowledge of dynamically significant meteorological features, such as ARs, the upper-level jet, and cold-air troughs, has been fundamental to planning each mission's flight tracks during AR Recon.

During the 2019 and 2020 seasons, adjoint sensitivity analysis was supplemented by ensemble-based sensitivity analysis of both the ECMWF and GFS models (Torn and Hakim 2008). Ensemble-based sensitivity analyses emphasize synoptic-scale differences between ensemble members that are associated with significant weather features at the initial time (Torn and Hakim 2008). Performing observation targeting based on independent sensitivity analysis methods increased confidence in the robustness of targeted regions of sensitivity. In the majority of cases both the adjoint and ensemble sensitivity analyses highlighted forecast sensitivity along the AR core, its edges, and in the warm conveyor belt. Within these cloudy and generally data-sparse regions of moisture convergence, subsequent precipitation and latent heating are known to influence frontogenesis (Lackmann 2002) and cyclogenesis (Davis 1992), which feed back into the evolution of water vapor transport (Lackmann 2002) and modify downstream precipitation impacts. Dropsonde data collected in these dynamically active regions is also valuable for evaluating model representation of the fundamental processes that govern AR evolution in global models (e.g., Neiman et al. 2016; Demirdjian et al. 2020a).

AR Recon implementation

Across all IOPs in the 2018, 2019, and 2020 seasons, reconnaissance considered meteorological features that the precipitation forecast sensitivity methods highlighted as the primary observation targets. These locations of maximum sensitivity were generally found in the subsaturated edges of AR cores (similar to Reynolds et al. 2019). Secondary targets included locations of low-level PV sensitivity maxima, which were typically found in the southeast quadrant of the cyclone associated with enhanced water vapor transport and convergence (e.g., Fig. 7a). Flight tracks for all available aircraft were optimized to sample these features broadly. For example, individual aircraft were stationed at Hickam Air Force Base (AFB) in Hawaii; Travis AFB in central California; and Tacoma, Washington, during the 2018 season (Fig. 1) to facilitate sampling the full AR structure as well as parent circulation features. The USAF C-130s stationed in Hawaii and California had a limited range (~5,500 km) relative to the NOAA G-IV that was stationed in Washington (~6,500 km). The G-IV's range, maximum altitude (~13,500 m) and more northern location best suited it to sampling dynamical features of the attendant cyclone, while the C-130s were tasked with sampling AR transects over the eastern Pacific. A U.S. Air Force Weather Officer and an Air Force Navigator were stationed at CW3E for the duration of the campaign to facilitate coordination between observational target goals and aircraft capabilities (Fig. 6). Individual aircraft were flexible in the number of dropsondes that they could deploy along-track, according to desired spacing and target size, though the average number per mission per aircraft was 25. Dropsondes were primarily released within the GFS data assimilation update cycle centered on 0000 UTC and spanning 2100–0300 UTC.

AR Recon 2018 consisted of six IOPs, three of which included both C-130s and the G-IV (Fig. 8). Unfortunately, strong blocking prevailed off the coast of California for the majority of the campaign period and resulted in IOPs with ARs that featured more anticyclonic vapor transport than is typically associated with extreme events in California (Fig. 8). The precipitation impacts of the IOP events primarily affected the Pacific Northwest. IOP-1 sampled a moderate-strength AR that extended from north of Hawaii (25°N, 160°W) to coastal Oregon (45°N, 125°W; Fig. 8a). The USAF C-130s stationed at Hickam AFB in Hawaii and Travis AFB in California sampled the tail and head of the AR, respectively. The NOAA G-IV deployed dropsondes across the middle segment of the AR, between C-130 tracks across the AR, and also sampled the dynamical features associated with the attendant low pressure system, which included a PV strip that precipitation forecasts were particularly sensitive to (Fig. 7b). The G-IV also performed GPS-ARO measurements during each of its three flights to augment the number of atmospheric profiles (Haase et al. 2014). Since the occultation profiles are oblique rather than vertical, they complement those available from dropsondes and significantly increase the observed area (Chen et al. 2018).

The 2019 campaign consisted of six IOPs as well, though only two C-130s were available for missions. Notably, this campaign year consisted of multiple impactful precipitation events for California, several of which have been developed as independent case studies (e.g., Cannon et al. 2020b). In addition to dropsonde observations over six IOPs, 32 drifting buoys with barometers were deployed by two C-130 flights in mid-January to substantially increase the number of pressure observations over the data-sparse northeast Pacific. These data have previously been shown to positively impact the representation of large-scale circulation in NWP (Centurioni et al. 2017; Ingleby and Isaksen 2018) and, in concert with targeted dropsondes, have the potential to improve AR forecast skill. A total of 15 IOPs were flown between the 2016, 2018, and 2019 campaigns (Fig. 8).

Seventeen IOPs flown between late-January and mid-March 2020 more than doubled the previous program total. An additional 64 drifting buoys with barometers were also deployed during the campaign season. Similar to 2018, a blocking high in the eastern Pacific led to a paucity of AR landfalls in California during 2020, though a series of impactful Pacific Northwest ARs were sampled. A notable change to the sampling strategy in 2020 was to consistently utilize the three aircraft (two C-130s and the G-IV) in a manner that enabled the same AR to be sampled on consecutive days prior to landfall (when the synoptic setup was conducive to doing so). This change was implemented in an effort to sustain dropsonde information in the forecast leading up to AR landfall, which was preliminarily shown to yield larger benefits than assimilating dropsondes in any single forecast cycle in previous years due to the e-folding time of the data impact (Black et al. 2017). The 32 IOPs flown to date comprise a substantial data sample for ongoing studies on the impacts of assimilating targeted observations on AR forecast skill, which are briefly introduced in the following section.

Data assimilation impact studies

Researchers at CW3E are currently working in partnership with individuals at NRL, NCEP, and ECMWF to perform data denial hindcasts using each center's global or regional model to quantify the added benefit of AR Recon dropsonde measurements. The collaboration has been formalized through the formation of the AR Recon Modeling and Data Assimilation Steering Committee (membership is listed in Table 2), which ensures cooperation between participating organizations in developing and executing a 5-yr work plan for AR Recon data assimilation efforts.

The dropsonde observations collected during AR Recon define both the horizontal and vertical structure of ARs, enabling model assessment (e.g., Schäfler et al. 2018) and data impact studies (e.g., Majumdar 2016). Lavers et al. (2018) performed a detailed analysis of ensemble data assimilation in the ECMWF IFS using AR Recon 2018 dropsonde observations and concluded that although the structure of ARs is well represented by the forecast model,

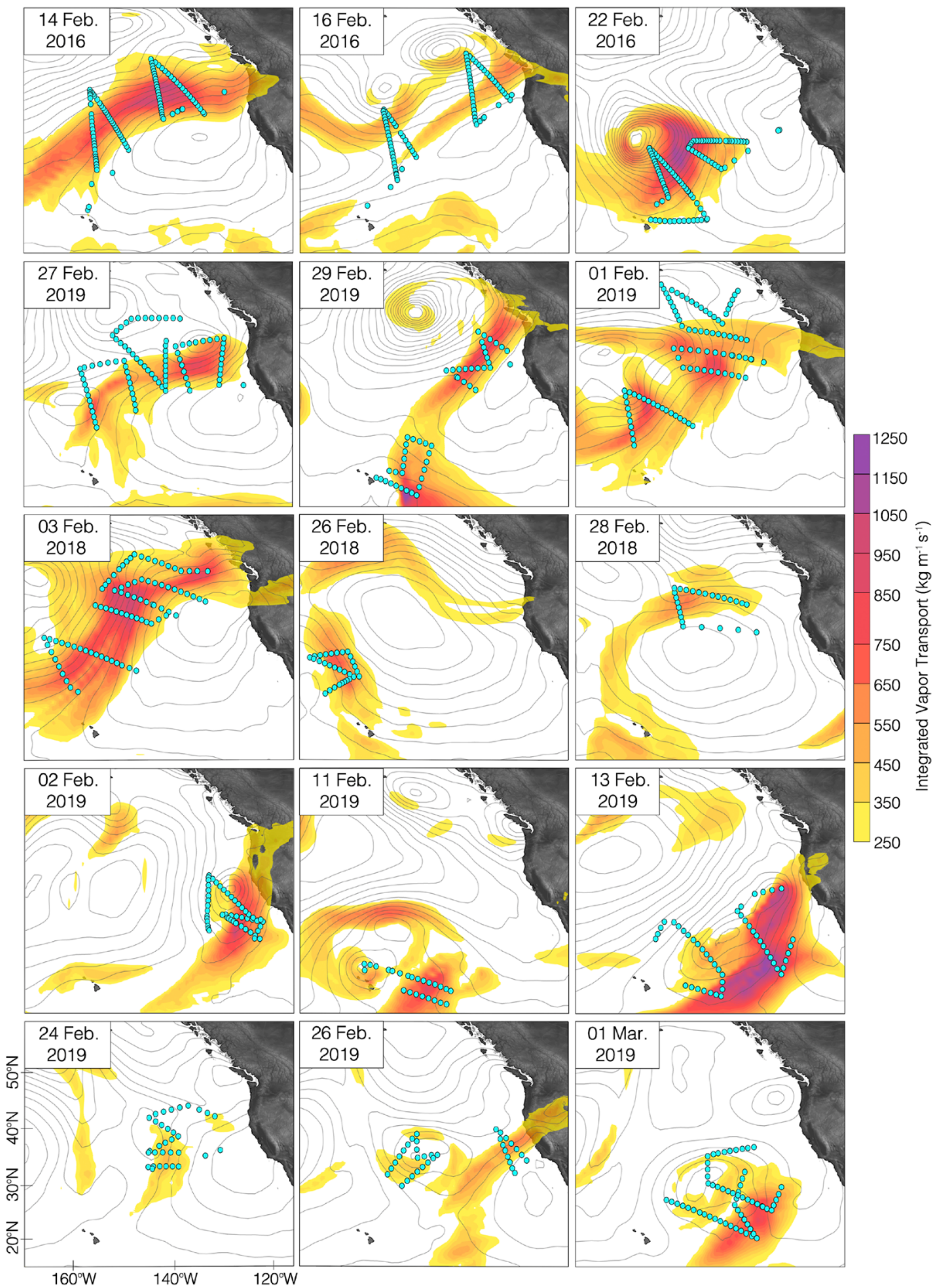

Fig. 8. IVT (color shading), sea level pressure (contours), and dropsonde locations (cyan symbols) for each IOP during the 2016, 2018, and 2019 campaigns.

Table 2. AR Recon modeling and data assimilation steering committee membership.

Name	Title	Institution	Role
F. Martin Ralph	Director, Center for Western Weather and Water Extremes	Scripps Institution of Oceanography, UC San Diego	AR Recon PI and steering committee co-chair
Vijay Tallapragada	Chief, Modeling and Data Assimilation Branch, National Centers for Environmental Prediction	National Oceanic and Atmospheric Administration	AR Recon co-PI and steering committee co-chair
James Doyle	Senior Scientist, Marine Meteorology Division	Naval Research Laboratory	AR Recon adjoint modeling lead and steering committee member
Aneesh Subramanian	Assistant Professor	University of Colorado Boulder	AR Recon data assimilation lead and steering committee member
Luca Delle Monache	Deputy Director, Center for Western Weather and Water Extremes	Scripps Institution of Oceanography, UC San Diego	Data assimilation steering committee member
Chris Davis	Associate Director, Mesoscale and Microscale Meteorology Laboratory	National Center for Atmospheric Research	AR Recon observation targeting lead and steering committee member
Florian Pappenberger	Director of Forecasts	European Centre for Medium-Range Weather Forecasts	Data assimilation steering committee member

significant errors exist in the simulation of IVT that originate largely from the winds above the planetary boundary layer. Furthermore, errors in the specific humidity at 850 hPa can cause large IVT uncertainties. These issues may then result in errors in the location of low-level water vapor as well as in its condensation and resulting latent heat release, which in turn affects atmospheric dynamics and predictability (Lackmann 2002; Schäfler et al. 2018). Thus, assimilated dropsonde observations are expected to reduce IVT uncertainties and may improve forecasts of subsequent high-impact precipitation events.

Historically, dropsonde observations have been key to hurricane prediction and are frequently employed as part of national weather operations to improve tropical cyclone track forecasts (Aberson 2011; Reynolds et al. 2013; Majumdar 2016). Previous studies that have investigated the impact of dropsonde assimilation on tropical cyclone forecasts have exhibited reductions in track forecast error of up to 20%–40%, depending on the forecasting system (Wu et al. 2007). The reduced impact of dropsonde assimilation on tropical cyclone track forecasts in the ECMWF IFS reported by Weissmann et al. (2011) is potentially a result of the advanced 4D-VAR assimilation of satellite data and the improved baseline forecast provided by that model, which reduced the potential for large gains from assimilating supplemental observations (Majumdar et al. 2016). On the other hand, data assimilation systems have continued to improve through, for example, the use of flow-dependent covariances and better treatment of observation and representation errors which should lead to an increased impact of observations (Schindler et al. 2020). The dichotomy of recent results underscores the challenge of demonstrating that supplemental observations have a significant impact on the forecasts of modern operational NWP systems. A number of previous studies have had limited success in identifying the impact of targeted observations on forecast skill due to issues including observation error, targeting strategy, numerical modeling, assimilation technique and verification methodology (Buizza et al. 2007; Romine et al. 2016; Majumdar 2016).

The concept of improving forecast accuracy through targeted observations has also been applied to winter storms in the Fronts and Atlantic Storm Track Experiment (FASTEX; Joly et al. 1999) and The Observing System Research and Predictability Experiment (THORPEX: 2017) with weaker than anticipated impact. However, dropsonde observations from the NAWDEX campaign improved the operational ECMWF forecast system up to 3% over the course of the campaign, with individual short-range forecasts improving up to 30% (Schindler et al. 2020). Similarly, Stone et al. (2020) demonstrated that AR Recon dropsondes had a per-observation impact 2 times larger than that of the baseline downstream radiosonde network across four 2018 cases. Thus, continued research that acknowledges and learns from the limitations encountered in early studies to develop targeting strategies and data assimilation methodologies that are better adapted to supplemental observations are critical to demonstrating the benefit of AR Recon. Additionally, the physical processes in AR environments and forecast needs of regional stakeholders pose a different set of challenges for predictability and observation targeting than those that exist for tropical cyclones, and as a result it is imperative that targeting and assimilation for AR Recon be carried out with sufficient flexibility and independence to adapt to the uniqueness of West Coast weather and climate.

During AR Recon 2018, 2019, and 2020, dropsonde data were ingested into the operational GFS, NRL, and ECMWF data assimilation systems in real time (Table 3; records of assimilated data are incomplete for 2016). The 80–87 assimilated dropsondes from three aircraft in IOP1 2018, for example, accounted for the majority of in situ sounding profiles over the oceans and nearly 10% of all in situ profiles in each model, globally (Fig. 9). In regions with deep clouds and precipitation, where all-sky radiance data have comparatively large errors (English et al. 2013), dropsondes provide unique information on the vertical profile of the atmosphere.

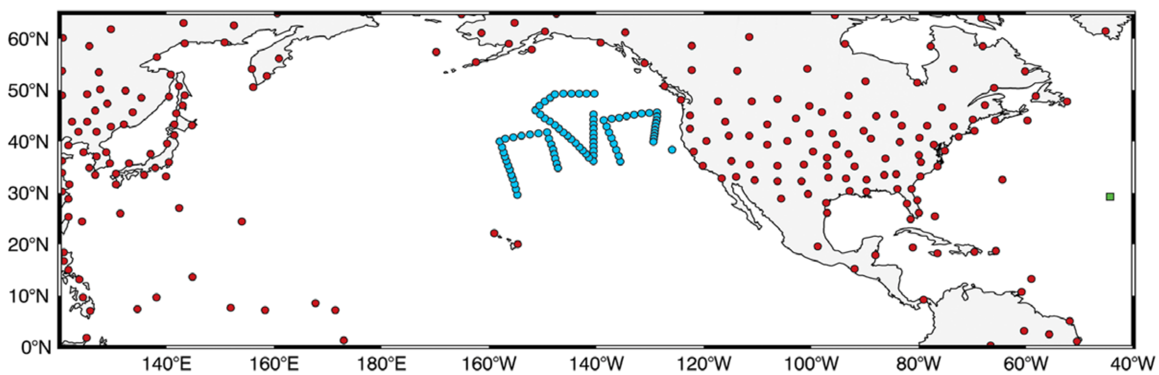

Fig. 9. Locations of assimilated data at 0000 UTC 27 Jan 2018 from the ECMWF forecasting system. Red dots identify the global radiosonde network, green dots identify ship-based soundings, and blue dots identify observations from AR Recon aircraft.

Data denial experiments that systematically withhold particular observations from the assimilation system to produce otherwise identical experiments with varying initial states are necessary to evaluate the impact of those observations on forecast skill (e.g., Romine et al. 2016). These simulations are currently under development at CW3E using the community gridpoint statistical interpolation analysis system (GSI) and West-WRF, a version of the Weather Research and Forecasting (WRF) Model that was configured to optimally represent ARs and wintertime meteorology on the West Coast (Martin et al. 2018). In these assimilation experiments, dropsonde data are ingested into the WRF forecast model using the GSI hybrid four-dimensional ensemble-variational (4D EnVar) method to systematically evaluate their impact on forecast skill relative to other routinely assimilated data, including satellite atmospheric motion vector winds and all-sky radiances (English et al. 2013). Preliminary results have demonstrated significant improvements in AR landfall skill at short-to-moderate lead times that are attributable to improved representation of AR conditions in the model's initial state in specific IOP case studies. Figure 10 shows that assimilating dropsonde observations generate large differences in the model's initial conditions and lead to an overall reduction in West-WRF initial condition uncertainty (as measured by the difference between the West-WRF and GFS analyses). Notably, the underestimation of IVT amplitude in IOP 1 near 40°N, 150°W—a key region of precipitation forecast sensitivity to humidity perturbations in the COAMPS adjoint simulation for that case (Fig. 7a)—is minimized in the WithDrop simulation (Fig. 10b) relative to the NoDrop

Table 3. AR Recon IOPs, aircraft, and assimilated dropsonde statistics.

Date	AF C-130	AF C-130	NOAA G-IV	Dropsondes	Dropsondes assimilated		
					NCEP	ECMWF	Navy
2016							
0000 UTC 14 Feb	×	×	*	99	69	**	**
0000 UTC 16 Feb	×	×	*	80	42	**	**
0000 UTC 22 Feb	×	×	*	95	46	**	**
2018							
0000 UTC 27 Jan	×	×	×	88	87	80	87
0000 UTC 29 Jan	×	×		49	47	41	47
0000 UTC 1 Feb	×	×	×	90	88	79	88
0000 UTC 3 Feb	×	×	×	89	86	86	86
0000 UTC 26 Feb	×			30	0	0	0
0000 UTC 28 Feb	×			25	25	25	25
2019							
0000 UTC 2 Feb	×	×		60	58	52	53
0000 UTC 11 Feb	×			26	24	24	24
0000 UTC 13 Feb	×	×		53	47	48	40
0000 UTC 24 Feb	×	×		52	45	44	45
0000 UTC 26 Feb	×	×		36	35	35	35
0000 UTC 1 Mar	×	×		64	47	54	59
2020							
0000 UTC 24 Jan	×	×		37	37	33	37
0000 UTC 29 Jan	×	×		27	21	23	25
0000 UTC 31 Jan	×			24	24	22	24
0000 UTC 4 Feb	×	×	×	70	70	65	70
0000 UTC 5 Feb			×	30	30	30	30
0000 UTC 6 Feb	×	×	×	77	59	54	59
0000 UTC 14 Feb			×	30	27	28	30
0000 UTC 15 Feb	×	×	×	78	78	73	78
0000 UTC 16 Feb			×	30	30	27	30
0000 UTC 21 Feb			×	30	29	26	29
0000 UTC 24 Feb	×		×	55	55	50	55
0000 UTC 2 Mar	×	×	×	77	74	72	74
0000 UTC 7 Mar			×	30	30	26	30
0000 UTC 8 Mar	×		×	55	54	49	54
0000 UTC 9 Mar		×	×	29	29	26	29
0000 UTC 10 Mar	×		×	52	39	51	52
0000 UTC 11 Mar		×		2	2	2	2

* During 2016 the NOAA G-IV and NASA Global Hawk conducted research flights as part of the NOAA El Niño Rapid Response (ENRR) field campaign. The Global Hawk partially sampled ARs in coordination with the AR Recon C-130s. The G-IV sampled tropical conditions south of Hawaii based on ENRR's primary airborne objectives, which focused on tropical convection.

** The number of assimilated drops in the ECMWF and Navy models is not available for the 2016 season.

simulation (Fig. 10a). Subsequent improvements in AR and precipitation forecast skill over the duration of the event are the subject of continued research.

Identifying the impact of AR Recon dropsonde observations across the growing sample of IOPs is ongoing and fundamental to establishing the long-term benefit of the campaign. Accordingly, NCEP is currently performing dropsonde data denial experiments using the operational GFS system that fully cycle all other observations assimilated into the forecast (e.g., both conventional observations and satellite radiances) for the 2018, 2019, and 2020 seasons. Additionally, forecast sensitivity observation impact (FSOI) studies have been carried out at NRL using the Navy Global Environmental Model (NAVGEM) system, which demonstrated that AR reconnaissance dropsondes had significant beneficial impact, with per observation impact more than double that of the global radiosonde network across four cases in 2018 (Stone et al. 2020). The work of Stone et al. (2020) also identified model biases and potential issues with assumed error variances in the data assimilation system that could be remedied for the model to further benefit from assimilating targeted dropsondes (Stone et al. 2020). Furthermore, the positive impact of targeted dropsonde observations demonstrated by Kren et al. (2018) and Schindler et al. (2020) for extratropical cyclone forecasts in other campaigns, and their respective efforts to address existing limitations in operational data assimilation systems, bolster the argument for continued investment toward reconnaissance flights and advancing NWP capabilities to benefit from their data.

Vision of annual implementation

AR Recon and the formation of the Modeling and Data Assimilation Steering Committee have established a framework to address a need for improved West Coast precipitation forecast skill. AR Recon 2016, 2018, 2019, and 2020 demonstrated the successful implementation of the program and ongoing research is now illustrating its potential for positive impact on NWP. Given that NWP is an initial value problem that stands to benefit from improved observation of

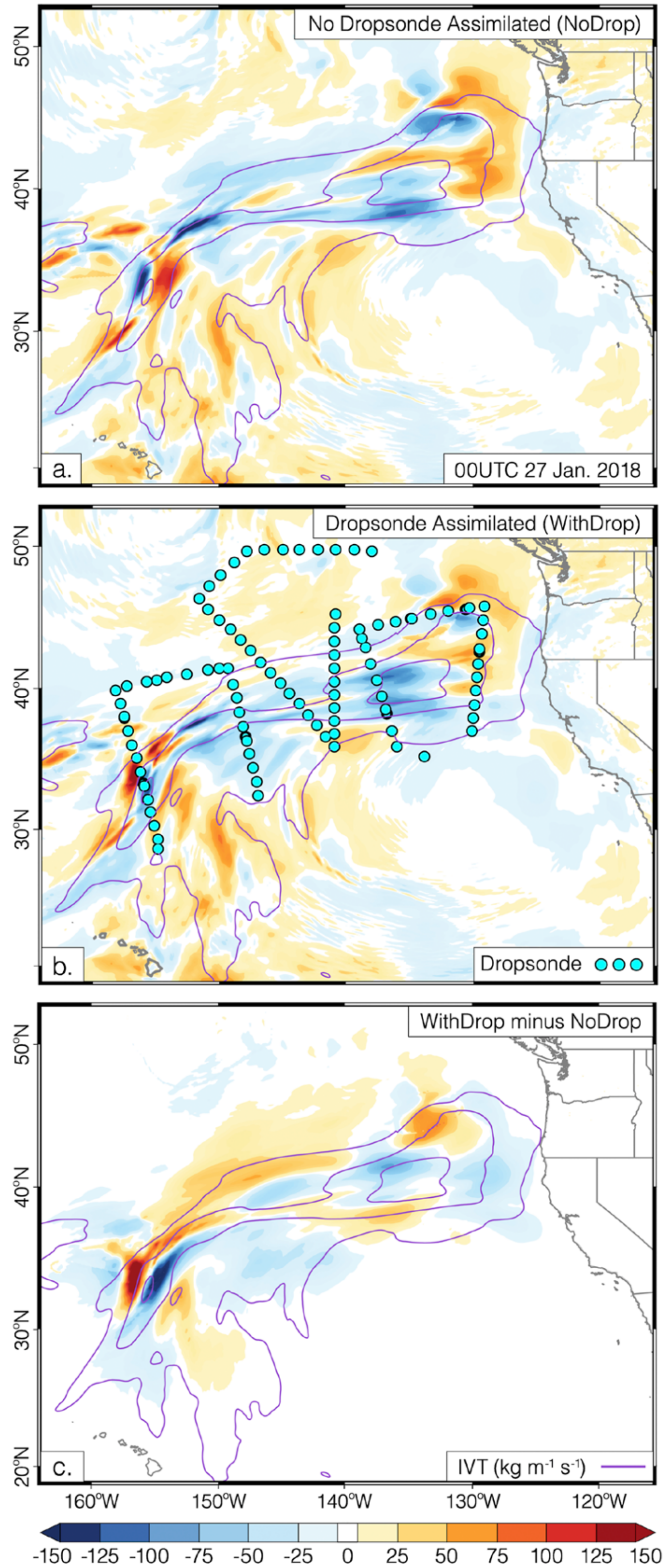

Fig. 10. IVT initial-condition error (color fill) in the West-WRF experiment (a) without assimilated dropsondes (NoDrop) and (b) with assimilated dropsondes (WithDrop) valid at 0000 UTC 27 Jan 2018. (c) IVT amplitude differences (color fill) between WithDrop and NoDrop. The purple contours in each panel identify the GFS analysis IVT, which is used to calculate the error. The contour starts from 250 kg m^{-1} s^{-1} with an increment of 250 kg m^{-1} s^{-1}. The first guess is initialized at 1800 UTC 26 Jan 2017.

the atmosphere, in both theory and practice, it is ideal that the sampling campaign continue on an annual basis—such an investment in a growing number of missions is fundamental to developing a sufficiently large dataset for the robust statistical evaluation of the added benefit of dropsonde observations to precipitation forecast skill (Kren et al. 2018).

Considerable effort is still required to quantify the impact of assimilating targeted dropsonde observations of offshore ARs on forecast skill and the potential for enhanced prediction of West Coast extreme weather events through the annual implementation of AR Recon. However, recent positive results (e.g., Stone et al. 2020) and the potential societal benefits of observing AR properties ahead of landfall warrants a considerable investment of aircraft, instrumentation, and research resources at the national level. Given that the aircraft used in AR Recon are typically designated for hurricane observations in the summer and fall, and are not already assigned to specific missions in the winter, these resources could be devoted to supporting West Coast meteorology and forecasting at that time of the year without compromising other important objectives. Ideally, the allocation of aircraft time on a year-to-year basis will be replaced by a permanent commitment of dedicated resources that is similar to national hurricane forecasting operations. A key step in this direction is the inclusion of AR Recon into the OFCM's Winter Season Operations Plan (OFCM 2019), which now specifically calls for airborne reconnaissance of atmospheric rivers. It is envisioned that the consistent commitment of resources to AR reconnaissance, and continued development of methodologies to assimilate collected data, would yield substantial returns for weather forecasting, water management, and hazard mitigation in the western United States. Furthermore, addressing drought and flooding challenges through improved forecasting and water management will be essential to enhancing western U.S. resiliency to climate change impacts in the coming decades.

Summary

Precipitation from atmospheric rivers (ARs) is the primary driver of regional water resources and weather-related hazards over the U.S. West Coast. Although there is a dearth of AR observations through the full troposphere ahead of landfall, forecasting of these features can be more skillful at long lead times than precipitation alone (Lavers et al. 2016) and can be leveraged to increase forecast lead time of high-impact events, though important forecast challenges remain at 0–4-day lead times. To provide increasingly skillful forecasts of ARs and their associated impacts on the spatial and temporal scales that are relevant to regional stakeholders, improved observations ahead of landfall are required, including through airborne observation campaigns (Doyle et al. 2014; Ralph et al. 2014; Neiman et al. 2016; Cordeira et al. 2017). The Atmospheric River Reconnaissance (AR Recon) campaign that was operational during winters 2016, 2018, 2019, and 2020 represents an important research and operations partnership between multiple academic institutions, state, federal and international agencies, and stakeholders toward improving forecast skill in the western United States. AR Recon is now transitioning into an operational mode that enhances the deep linkage between research and operations and the culture of collaboration that has formed the core of AR Recon development.

AR Recon has supported improved prediction of landfalling ARs on the U.S. West Coast by supplementing conventional data coverage with dropsonde observations of atmospheric profiles within ARs, GPS-ARO observations of oblique atmospheric profiles providing information about temperature and moisture, and surface pressure measurements from drifting buoys. The 2016, 2018, 2019, and 2020 campaigns consisted of a combination of three aircraft that were available to execute IOPs between January and March of each campaign year, respectively. For the 2018–20 campaigns, daily forecast briefings were conducted at Scripps and included participation from a range of experts as well as experienced weather officers and navigators from the U.S. Air Force and NOAA. In the event of predicted AR landfall impacts, NRL's COAMPS moist adjoint model was run to evaluate sensitivity of precipitation to initial conditions and to identify sensitive regions and targeted observing strategies. In total, 1,657 dropsondes have been deployed into and around AR conditions during 32 IOPs over four AR Recon seasons. The development of methodologies to effectively assimilate these airborne observations, and analysis of the impact of the data on those simulations, are ongoing and will be completed over the coming years in collaboration with NOAA/NCEP, ECMWF, and NRL as part of the AR Recon Modeling and Data Assimilation Steering Committee objectives. Table 4 synthesizes AR Recon programmatic milestones achieved since the project's inception in 2016 through the 2020 season.

While improved initial conditions for offshore water vapor, wind, pressure, and temperature are expected to positively impact the prediction of AR landfall and quantitative precipitation simulation at short-to-medium lead times, and recent studies using these data have demonstrated positive impacts in operational forecast systems (e.g., Stone et al. 2020), the dropsonde observations are also key to better understanding the dynamical processes that define AR characteristics, such as their strength, position, length, orientation, and duration, and identifying and mitigating data assimilation and forecast model deficiencies. Advancements in the fundamental science related to ARs, made possible through unique data from airborne reconnaissance, will also benefit numerical weather prediction (NWP) data assimilation and

Table 4. Major milestones in the development of AR Recon.

Milestones	2016	2017	2018	2019	2020
U.S. Army Corps of Engineers begins support of AR Recon through the CW3E Forecast Informed Reservoir Operations Program	×				
First dedicated AR Recon flights in partnership with NCEP, with 2 USAF C-130 aircraft: 6 total flights and 272 dropsondes released	×				
Assessment of lessons learned in 2016, and planning for 2018 season		×			
AR Recon 2016 data help define AR dynamics and kinematics in the American Meteorological Society *Glossary of Meteorology* (Ralph et al. 2018)		×			
California Department of Water Resources begins support of AR Recon through the CW3E AR Research Program		×			
Second AR Recon season, including support from the NOAA G-IV aircraft and 2 USAF C-130s: 13 total flights and 361 dropsondes released			×		
AR Recon Modeling and Data Assimilation Steering Committee formed			×		
Use of NRL COAMPS adjoint model to inform flight targeting			×	×	×
GPS-Radio Occultation deployment on NOAA G-IV or USAF C-130			×	×	×
Interagency workshops at ECMWF, NCEP, CW3E			×	×	×
Publication using dropsonde observations to document errors in ECMWF data assimilation first guess fields in AR conditions (Lavers et al. 2018)			×		
Third AR Recon season, with 2 C-130s: 9 total flights and 291 dropsondes				×	
Deployment of drifting buoys with partners at Scripps and ECMWF				×	×
Data denial runs completed at NRL, ECMWF, NCEP, NCAR, and CW3E, and preliminary assessment of AR Recon forecast impacts				×	×
AR Recon called for in OFCM's National Winter Season Operations Plan				×	
Congress appropriates funds in NOAA for AR Recon G-IV and NCEP				×	×
Stone et al. (2020) found impact of AR Recon in the NAVGEM forecast model was similar to that of entire North American Radiosonde network					×
Congress appropriates funds in Air Force for AR Recon					×
Fourth AR Recon season. Two C-130s and the NOAA G-IV flew 17 IOPs and released a total of 733 dropsondes					×
Planned: AR Recon 2021 from 8 January to 31 March, 3 aircraft					

model system development as well as forecasting of these features (e.g., Martin et al. 2018). Given that NWP is an initial value problem that benefits from reducing analysis error, and the need for better understanding AR dynamics and forecast challenges, AR Recon's ongoing scientific commitments and recent inclusion into the National Winter Season Operations Plan (OFCM 2019) are expected to result in substantially improved outcomes for water management and emergency preparedness in the West.

Acknowledgments. This research was supported the U.S. Army Corps of Engineers (USACE) as part of Forecast Informed Reservoir Operations (FIRO) under Grant W912HZ-15-2-0019. Additional funding was provided by the California Department of Water Resources. Doyle and Reynolds acknowledge the support by the Chief of Naval Research through the NRL Base Program Program Element (PE) 0601153N, and Office of Naval Research PE 0601153N. The primary facilities partners that have made AR Recon possible are the U.S. Air Force 53rd Weather Reconnaissance Squadron, and the NOAA Aircraft Operations Center. AR Recon would not be possible without the outstanding effort of the flight crews in planning and executing targeted observation missions.

References

Aberson, S. D., 2011: The impact of dropwindsonde data from the THORPEX–Pacific area regional campaign and the NOAA hurricane field program on tropical cyclone forecasts in the global forecasting system. *Mon. Wea. Rev.*, **139**, 2689–2703, https://doi.org/10.1175/2011MWR3634.1.

Amerault, C., X. Zou, and J. D. Doyle, 2008: Tests of an adjoint mesoscale model with explicit moist physics on the cloud scale. *Mon. Wea. Rev.*, **136**, 2120–2132, https://doi.org/10.1175/2007MWR2259.1.

Black, P., L. Harrison, M. Beaubien, R. Bluth, R. Woods, A. Penny, R. W. Smith, and J. D. Doyle, 2017: High-Definition Sounding System (HDSS) for atmospheric profiling. *J. Atmos. Oceanic Technol.*, **34**, 777–796, https://doi.org/10.1175/JTECH-D-14-00210.1.

Buizza, R., C. Cardinali, G. Kelly, and J.-N. Thépaut, 2007: The value of observations. II: The value of observations located in singular-vector-based target areas. *Quart. J. Roy. Meteor. Soc.*, **133**, 1817–1832.

Cannon, F., F. M. Ralph, A. M. Wilson, and D. P. Lettenmaier, 2017: GPM satellite radar measurements of precipitation and freezing level in atmospheric rivers: Comparison with ground-based radars and reanalyses. *J. Geophys. Res. Atmos.*, **122**, 12 747–12 764, https://doi.org/10.1002/2017JD027355.

——, C. W. Hecht, J. M. Cordeira, and F. M. Ralph, 2018: Synoptic and mesoscale forcing of Southern California extreme precipitation. *J. Geophys. Res. Atmos.*, **123**, 13 714–13 730, https://doi.org/10.1002/2017JD027355.

——, J. M. Cordeira, C. W. Hecht, J. R. Norris, A. Michaelis, R. Demirdjian, and F. M. Ralph, 2020a: GPM satellite radar observations of precipitation mechanisms in atmospheric rivers. *Mon. Wea. Rev.*, **148,** 1449–1463, https://doi.org/10.1175/MWR-D-19-0278.1.

——, and Coauthors, 2020b: Observations and predictability of an impactful narrow cold-frontal rainband over Southern California. *Wea. Forecasting*, https://doi.org/10.1175/WAF-D-20-0012.1, in press.

Centurioni, L., A. Horaìnyi, C. Cardinali, E. Charpentier, and R. Lumpkin, 2017: A global ocean observing system for measuring sea level atmospheric pressure: Effects and impacts on numerical weather prediction. *Bull. Amer. Meteor. Soc.*, **98**, 231–238, https://doi.org/10.1175/BAMS-D-15-00080.1.

Chen, X. M., and Coauthors, 2018: The impact of airborne radio occultation observations on the simulation of Hurricane Karl (2010). *Mon. Wea. Rev.*, **146**, 329–350, https://doi.org/10.1175/MWR-D-17-0001.1.

Cordeira, J. M., F. M. Ralph, A. Martin, N. Gaggini, J. R. Spackman, P. J. Neiman, J. J. Rutz, and R. Pierce, 2017: Forecasting atmospheric rivers during CalWater 2015. *Bull. Amer. Meteor. Soc.*, **98**, 449–459, https://doi.org/10.1175/BAMS-D-15-00245.1.

Corringham, T. W., F. M. Ralph, A. Gershunov, D. R. Cayan, and C. A. Talbot, 2019: Atmospheric rivers drive flood damages in the western United States. *Sci. Adv.*, **5**, eaax4631, https://doi.org/10.1126/sciadv.aax4631.

Davis, C. A., 1992: A potential-vorticity diagnosis of the importance of initial structure and condensational heating in observed extratropical cyclogenesis. *Mon. Wea. Rev.*, **120**, 2409–2428, https://doi.org/10.1175/1520-0493(1992)120<2409:APVDOT>2.0.CO;2.

DeFlorio, M., D. Waliser, B. Guan, D. Lavers, F. M. Ralph, and F. Vitart, 2018: Global assessment of atmospheric river prediction skill. *J. Hydrometeor.*, **19**, 409–426, https://doi.org/10.1175/JHM-D-17-0135.1.

Demirdjian, R., J. R. Norris, A. Martin, and F. M. Ralph, 2020a: Dropsonde observations of the ageostrophy within the pre-cold-frontal low-level jet associated with atmospheric rivers. *Mon. Wea. Rev.*, **148,** 1389–1406, https://doi.org/10.1175/MWR-D-19-0248.1.

——, J. D. Doyle, C. A. Reynolds, J. R. Norris, A. C. Michaelis, and F. M. Ralph, 2020b: A case study of the physical processes associated with the atmospheric river initial-condition sensitivity from an adjoint model. *J. Atmos. Sci.*, **77**, 691–709, https://doi.org/10.1175/JAS-D-19-0155.1.

Dettinger, M. D., 2013: Atmospheric Rivers as Drought Busters on the U.S. West Coast. *J. Hydrometeor.*, **14**, 1721–1732, https://doi.org/10.1175/JHM-D-13-02.1.

Doyle, J. D., C. A. Reynolds, C. Amerault, and J. Moskaitis, 2012: Adjoint sensitivity and predictability of tropical cyclogenesis. *J. Atmos. Sci.*, **69**, 3535–3557, https://doi.org/10.1175/JAS-D-12-0110.1.

——, C. Amerault, C. A. Reynolds, and P. A. Reinecke, 2014: Initial condition sensitivity and predictability of a severe extratropical cyclone using a moist adjoint. *Mon. Wea. Rev.*, **142**, 320–342, https://doi.org/10.1175/MWR-D-13-00201.1.

——, C. A. Reynolds, and C. Amerault, 2019: Adjoint sensitivity analysis of high-impact extratropical cyclones. *Mon. Wea. Rev.*, **147**, 4511–4532, https://doi.org/10.1175/MWR-D-19-0055.1.

English, S., and Coauthors, 2013: Impact of satellite data. ECMWF Tech. Memo. 711, 46 pp., https://doi.org/10.21957/b6596ot1s.

Errico, R. M., 1997: What is an adjoint model? *Bull. Amer. Meteor. Soc.*, **78**, 2577–2591, https://doi.org/10.1175/1520-0477(1997)078<2577:WIAAM>2.0.CO;2.

Forecast Informed Reservoir Operations Steering Committee, 2017: Preliminary viability assessment of Lake Mendocino. Scripps Institution of Oceanography, 75 pp., accessed 2 April 2018, http://escholarship.org/uc/item/66m803p2.

Guan, B., and D. E. Waliser, 2015: Detection of atmospheric rivers: Evaluation and application of an algorithm for global studies. *J. Geophys. Res. Atmos.*, **120**, 12 514–12 535, https://doi.org/10.1002/2015JD024257.

Haase, J. S., B. J. Murphy, P. Muradyan, F. G. Nievinski, K. M. Larson, J. L. Garrison, and K.-N. Wang, 2014: First results from an airborne GPS radio occultation system for atmospheric profiling. *Geophys. Res. Lett.*, **41**, 1759–1765, https://doi.org/10.1002/2013GL058681.

Hamill, T. M., F. Yang, C. Cardinali, and S. J. Majumdar, 2013: Impact of targeted winter storm reconnaissance dropwindsonde data on midlatitude numerical weather predictions. *Mon. Wea. Rev.*, **141**, 2058–2065, https://doi.org/10.1175/MWR-D-12-00309.1.

Henn, B., R. Weihs, A. C. Martin, F. M. Ralph, and T. Osborne, 2020: Skill of rain-snow level forecasts for landfalling atmospheric rivers: A multimodel assessment using California's network of vertically profiling radars. *J. Hydrometeor.*, **21**, 751–771, https://doi.org/10.1175/JHM-D-18-0212.1.

Ingleby, B., and L. Isaksen, 2018: Drifting buoy pressures: Impact on NWP. *Atmos. Sci. Lett.*, **19**, e822, https://doi.org/10.1002/asl.822.

Joly, A., and Coauthors, 1999: Overview of the field phase of the fronts and Atlantic Storm-Track EXperiment (FASTEX) project. *Quart. J. Roy. Meteor. Soc.*, **125**, 3131–3163, https://doi.org/10.1002/qj.49712556103.

Kren, A. C., L. Cucurull, and H. Wang, 2018: Impact of UAS global hawk dropsonde data on tropical and extratropical cyclone forecasts in 2016. *Wea. Forecasting*, **33**, 1121–1141, https://doi.org/10.1175/WAF-D-18-0029.1.

Lackmann, G. M., 2002: Cold-frontal potential vorticity maxima, the low-level jet, and moisture transport in extratropical cyclones. *Mon. Wea. Rev.*, **130**, 59–74, https://doi.org/10.1175/1520-0493(2002)130<0059:CFPVMT>2.0.CO;2.

Lavers, D. A., D. E. Waliser, F. M. Ralph, and M. D. Dettinger, 2016: Predictability of horizontal water vapor transport relative to precipitation: Enhancing situational awareness for forecasting western U.S. extreme precipitation and flooding. *Geophys. Res. Lett.*, **43**, 2275–2282, https://doi.org/10.1002/2016GL067765.

——, M. J. Rodwell, D. S. Richardson, F. M. Ralph, J. D. Doyle, C. A. Reynolds, V. Tallapragada, and F. Pappenberger, 2018: The gauging and modeling of rivers in the sky. *Geophys. Res. Lett.*, **45**, 7828–7834, https://doi.org/10.1029/2018GL079019.

Leung, L. R., and Y. Qian, 2009: Atmospheric rivers induced heavy precipitation and flooding in the western U.S. Simulated by the WRF regional climate model. *Geophys. Res. Lett.*, **36**, L03820, https://doi.org/10.1029/2008GL036445.

Majumdar, S. J., 2016: A review of targeted observations. *Bull. Amer. Meteor. Soc.*, **97**, 2287–2303, https://doi.org/10.1175/BAMS-D-14-00259.1.

Martin, A., F. M. Ralph, R. Demirdjian, L. DeHaan, R. Weihs, J. Helly, D. Reynolds, and S. Iacobellis, 2018: Evaluation of atmospheric river predictions by the WRF Model using aircraft and regional Mesonet observations of orographic precipitation and its forcing. *J. Hydrometeor.*, **19**, 1097–1113, https://doi.org/10.1175/JHM-D-17-0098.1.

Nardi, K. M., E. A. Barnes, and F. M. Ralph, 2018: Assessment of numerical weather prediction model reforecasts of the occurrence, intensity, and location of atmospheric rivers along the West Coast of North America. *Mon. Wea. Rev.*, **146**, 3343–3362, https://doi.org/10.1175/MWR-D-18-0060.1.

Neiman, P. J., F. M. Ralph, G. A. Wick, J. D. Lundquist, and M. D. Dettinger, 2008: Meteorological characteristics and overland precipitation impacts of atmospheric rivers affecting the West Coast of North America based on eight years of SSM/I satellite observations. *J. Hydrometeor.*, **9**, 22–47, https://doi.org/10.1175/2007JHM855.1.

——, A. B. White, F. M. Ralph, D. J. Gottas, and S. I. Gutman, 2009: A water vapour flux tool for precipitation forecasting. *Water Manage.*, **162**, 83–94, https://doi.org/10.1680/WAMA.2009.162.2.83.

——, B. J. Moore, A. B. White, G. A. Wick, J. Aikins, D. L. Jackson, J. R. Spackman, and F. M. Ralph, 2016: An airborne and ground-based study of a long-lived and intense atmospheric river with mesoscale frontal waves impacting California during CalWater-2014. *Mon. Wea. Rev.*, **144**, 1115–1144, https://doi.org/10.1175/MWR-D-15-0319.1.

Oakley, N. S., F. Cannon, R. Munroe, J. T. Lancaster, D. Gomberg, and F. M. Ralph, 2018: Brief Communication: Meteorological and climatological conditions associated with the 9 January 2018 post-fire debris flows in Montecito and Carpinteria, California, USA. *Nat. Hazards Earth Syst. Sci.*, **18**, 3037–3043, https://doi.org/10.5194/nhess-18-3037-2018.

OFCM, 2019: National Winter Season Operations Plan (NWSOP). Office of the Federal Coordinator for Meteorological Services and Supporting Research, 84 pp., www.ofcm.gov/publications/nwsop/2019_nwsop.pdf.

Parsons, D. B., and Coauthors, 2017: THORPEX research and the science of prediction. *Bull. Amer. Meteor. Soc.*, **98**, 807–830, https://doi.org/10.1175/BAMS-D-14-00025.1.

Ralph, F. M., P. J. Neiman, and G. A. Wick, 2004: Satellite and CALJET aircraft observations of atmospheric rivers over the eastern North Pacific Ocean during the winter of 1997/98. *Mon. Wea. Rev.*, **132**, 1721–1745, https://doi.org/10.1175/1520-0493(2004)132<1721:SACAOO>2.0.CO;2.

——, P. J. Neiman, G. A. Wick, S. I. Gutman, M. D. Dettinger, D. R. Cayan, and A. B. White, 2006: Flooding on California's Russian River: Role of atmospheric rivers. *Geophys. Res. Lett.*, **33**, L13801, https://doi.org/10.1029/2006GL026689.

——, E. Sukovich, D. Reynolds, M. Dettinger, S. Weagle, W. Clark, and P. J. Neiman, 2010: Assessment of extreme quantitative precipitation forecasts and development of regional extreme event thresholds using data from HMT-2006 and COOP observers. *J. Hydrometeor.*, **11**, 1286–1304, https://doi.org/10.1175/2010JHM1232.1.

——, T. Coleman, P. J. Neiman, R. Zamora, and M. D. Dettinger, 2013: Observed impacts of duration and seasonality of atmospheric-river landfalls on soil moisture and runoff in coastal northern California. *J. Hydrometeor.*, **14**, 443–459, https://doi.org/10.1175/JHM-D-12-076.1.

——, and Coauthors, 2014: A vision for future observations for western U.S. extreme precipitation and flooding. *J. Contemp. Water Res. Educ.*, **153**, 16–32, https://doi.org/10.1111/J.1936-704X.2014.03176.X.

——, and Coauthors, 2016: CalWater field studies designed to quantify the roles of atmospheric rivers and aerosols in modulating U.S. West Coast precipitation in a changing climate. *Bull. Amer. Meteor. Soc.*, **97**, 1209–1228, https://doi.org/10.1175/BAMS-D-14-00043.1.

——, and Coauthors, 2017: Atmospheric rivers emerge as a global science and applications focus. *Bull. Amer. Meteor. Soc.*, **98**, 1969–1973, https://doi.org/10.1175/BAMS-D-16-0262.1.

——, M. D. Dettinger, M. M. Cairns, T. J. Galarneau, and J. Eylander, 2018: Defining "atmospheric river": How the *Glossary of Meteorology* helped resolve a debate. *Bull. Amer. Meteor. Soc.*, **99**, 837–839, https://doi.org/10.1175/BAMS-D-17-0157.1.

——, J. J. Rutz, J. M. Cordeira, M. Dettinger, M. Anderson, D. Reynolds, L. J. Schick, and C. Smallcomb, 2019: A scale to characterize the strength and impacts of atmospheric rivers. *Bull. Amer. Meteor. Soc.*, **100**, 269–289, https://doi.org/10.1175/BAMS-D-18-0023.1.

Reynolds, C. A., R. Langland, P. M. Pauley, and C. Velden, 2013: Tropical cyclone data impact studies: Influence of model bias and synthetic observations. *Mon. Wea. Rev.*, **141**, 4373–4394, https://doi.org/10.1175/MWR-D-12-00300.1.

——, J. D. Doyle, F. M. Ralph, and R. Demirdjian, 2019: Adjoint sensitivity of North Pacific atmospheric river forecasts. *Mon. Wea. Rev.*, **147**, 1871–1897, https://doi.org/10.1175/MWR-D-18-0347.1.

Romine, G. S., C. S. Schwartz, R. D. Torn, and M. L. Weisman, 2016: Impact of assimilating dropsonde observations from MPEX on ensemble forecasts of severe weather events. *Mon. Wea. Rev.*, **144**, 3799–3823, https://doi.org/10.1175/MWR-D-15-0407.1.

Rutz, J. J., W. J. Steenburgh, and F. M. Ralph, 2014: Climatological Characteristics of Atmospheric Rivers and Their Inland Penetration over the Western United States. *Mon. Wea. Rev.*, **142**, 905–921, https://doi.org/10.1175/MWR-D-13-00168.1.

Schäfler, A. G., and Coauthors, 2018: The North Atlantic waveguide and downstream impact experiment. *Bull. Amer. Meteor. Soc.*, **99**, 1607–1637, https://doi.org/10.1175/BAMS-D-17-0003.1.

Schindler, M., M. Weissmann, A. Schäfler, and G. Radnoti, 2020: The impact of dropsonde and extra radiosonde observations during NAWDEX in Autumn 2016. *Mon. Wea. Rev.*, **148**, 809–824, https://doi.org/10.1175/MWR-D-19-0126.1.

Schweiger, P., 2018: Lessons-to-be-learned from Oroville Dam spillway. *Seventh Int. Symp. on Hydraulic Structures,* Aachen, Germany, IAHR, 2 pp., https://doi.org/10.15142/T3SS8F.

Stone, R. E., C. A. Reynolds, J. D. Doyle, R. Langland, N. Baker, D. A. Lavers, and F. M. Ralph, 2020: Atmospheric river reconnaissance observation impact in the Navy global forecast system. *Mon. Wea. Rev.*, **148**, 763–782, https://doi.org/10.1175/MWR-D-19-0101.1.

Sukovich, E. M., F. M. Ralph, F. E. Barthold, D. W. Reynolds, and D. R. Novak, 2014: Extreme quantitative precipitation forecast performance at the weather prediction center from 2001 to 2011. *Wea. Forecasting*, **29**, 894–911, https://doi.org/10.1175/WAF-D-13-00061.1.

Torn, R. D., and G. J. Hakim, 2008: Ensemble-based sensitivity analysis. *Mon. Wea. Rev.*, **136**, 663–677, https://doi.org/10.1175/2007MWR2132.1.

Vano, J. A., M. D. Dettinger, R. Cifelli, D. Curtis, A. Dufour, K. Miller, J. R. Olsen, and A. M. Wilson, 2019: Hydroclimatic extremes as challenges for the water management community: Lessons from Oroville Dam and Hurricane Harvey [in "Explaining Extremes of 2017 from a Climate Perspective"]. *Bull. Amer. Meteor. Soc.*, **100** (1), S9–S14, https://doi.org/10.1175/BAMS-D-18-0219.1.

Weissmann, M., and Coauthors, 2011: The influence of assimilating dropsonde data on Typhoon track and midlatitude forecasts. *Mon. Wea. Rev.*, **139**, 908–920, https://doi.org/10.1175/2010MWR3377.1.

Wernli, H., S. Dirren, M. A. Liniger, and M. Zillig, 2002: Dynamical aspects of the life-cycle of the winter storm "Lothar" (24–26 December 1999). *Quart. J. Roy. Meteor. Soc.*, **128**, 405–429, https://doi.org/10.1256/003590002321042036.

White, A. B., D. J. Gottas, A. F. Henkel, P. J. Neiman, F. M. Ralph, and S. I. Gutman, 2010: Developing a performance measure for snow-level forecasts. *J. Hydrometeor.*, **11**, 739–753, https://doi.org/10.1175/2009JHM1181.1.

——, B. J. Moore, D. J. Gottas, and P. J. Neiman, 2019: Winter storm conditions leading to excessive runoff above California's Oroville dam during January and February 2017. *Bull. Amer. Meteor. Soc.*, **100**, 55–70, https://doi.org/10.1175/BAMS-D-18-0091.1.

Wick, G. A., P. J. Neiman, F. M. Ralph, and T. M. Hamill, 2013: Evaluation of forecasts of the water vapor signature of atmospheric rivers in operational numerical weather prediction models. *Wea. Forecasting*, **28**, 1337–1352, https://doi.org/10.1175/WAF-D-13-00025.1.

——, J. Dunion, and J. Walker, 2018: Sensing hazards with operational unmanned technology: Impact study of Global Hawk unmanned aircraft system observations for hurricane forecasting, final report. NOAA Tech. Memo. OAR-UAS-002, 92 pp., ftp://ftp1.esrl.noaa.gov/et6/sat/shout/data_impact/TM_SHOUT_Impact_Assessment_FINAL.pdf.

Wu, C. C., J.-H. Chen, P.-H. Lin, and K.-S. Chou, 2007: Targeted observations of tropical cyclones based on the adjoint-derived sensitivity steering vector. *J. Atmos. Sci.*, **64**, 2611–2626, https://doi.org/10.1175/JAS3974.1.

Zhu, Y., and R. E. Newell, 1998: A proposed algorithm for moisture fluxes from atmospheric rivers. *Mon. Wea. Rev.*, **126**, 725–735, https://doi.org/10.1175/1520-0493(1998)126<0725:APAFMF>2.0.CO;2.

——, and Coauthors, 2016: All-sky microwave radiance assimilation in NCEP's GSI analysis system. *Mon. Wea. Rev.*, **144**, 4709–4735, https://doi.org/10.1175/MWR-D-15-0445.1.